6° Prisma Day, Brembate di Sopra, 4-5 ottobre 2024

Ab initio strewn field for small asteroids impacts

A. Carbognani [1], M. Fenucci [2, 3], R. Salerno[4, 5], M. Micheli[2]

(1) INAF - Osservatorio di Astrofisica e Scienza dello Spazio, Via Gobetti 93/3, 40129 Bologna, Italy
(2) ESA ESRIN / PDO / NEO Coordination Centre, Largo Galileo Galilei, 1, 00044 Frascati (RM), Italy
(3) Elecnor Deimos, Via Giuseppe Verdi, 6, 28060 San Pietro Mosezzo (NO), Italy
(4) Meteo Expert, Via G. Marconi, 27, Segrate (MI) 20054, Italy
(5) Università Statale di Milano, Dipartimento di Scienze della Terra, Via S. Botticelli 23, Milano (MI) 20133, Italy

INAF
ISTITUTO NAZIONALE
DI ASTROFISICA

Prima Rete Italiana Sorveglianza Sistematica Meteore & Atmosfera
PRISMA

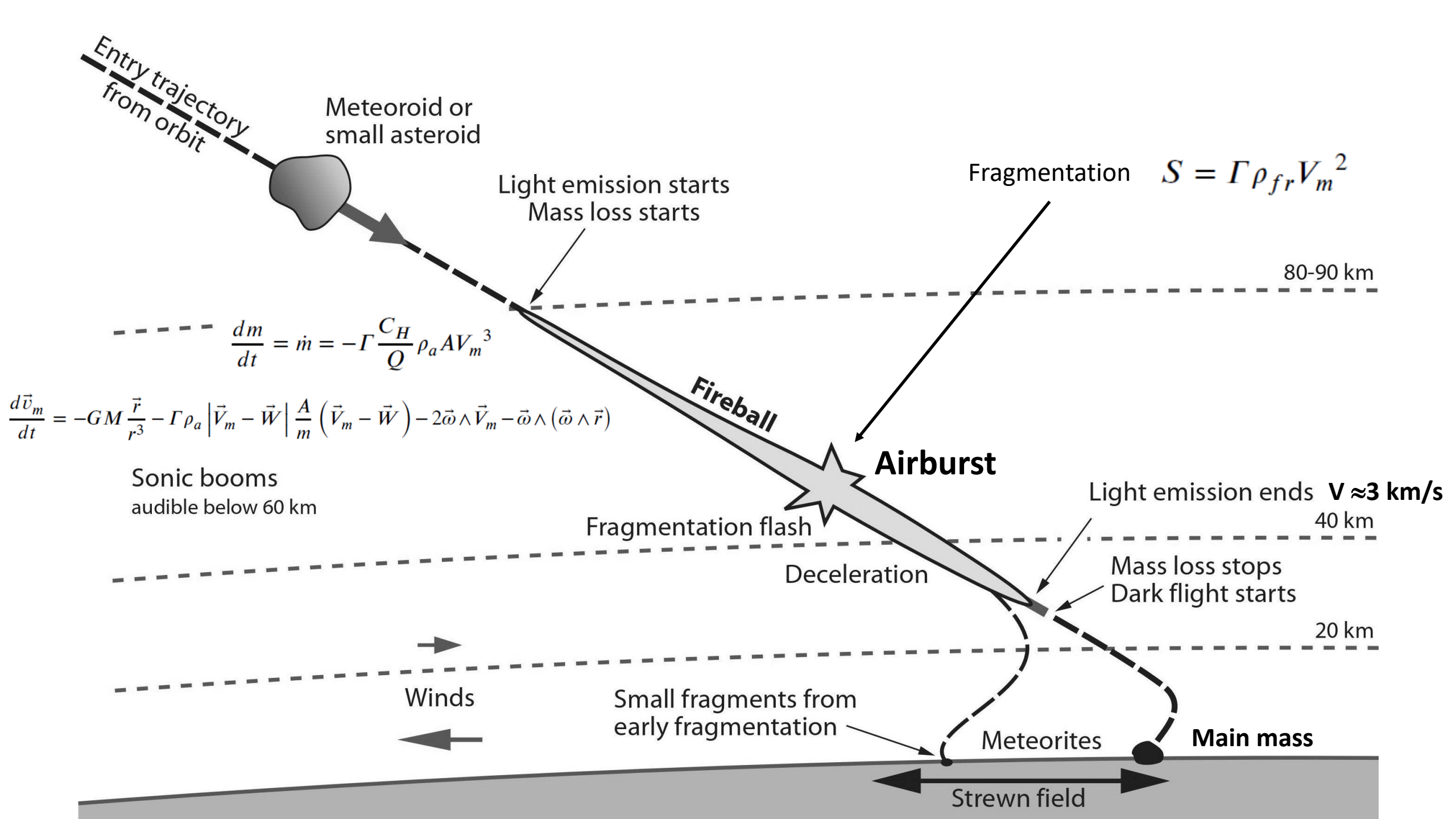
Entry trajectory from orbit
Meteoroid or small asteroid
Light emission starts
Mass loss starts
Fragmentation
$S = \Gamma \rho_{fr} V_m^2$
80-90 km
$\frac{dm}{dt} = \dot{m} = -\Gamma \frac{C_H}{Q} \rho_a A V_m^3$
$\frac{d\vec{v}_m}{dt} = -GM\frac{\vec{r}}{r^3} - \Gamma \rho_a \left|\vec{V}_m - \vec{W}\right| \frac{A}{m}\left(\vec{V}_m - \vec{W}\right) - 2\vec{\omega} \wedge \vec{V}_m - \vec{\omega} \wedge (\vec{\omega} \wedge \vec{r})$
Fireball
Airburst
Sonic booms
audible below 60 km
Light emission ends V ≈3 km/s
Fragmentation flash
40 km
Deceleration
Mass loss stops
Dark flight starts
20 km
Winds
Small fragments from early fragmentation
Meteorites
Main mass
Strewn field

Atmospheric Airbursts

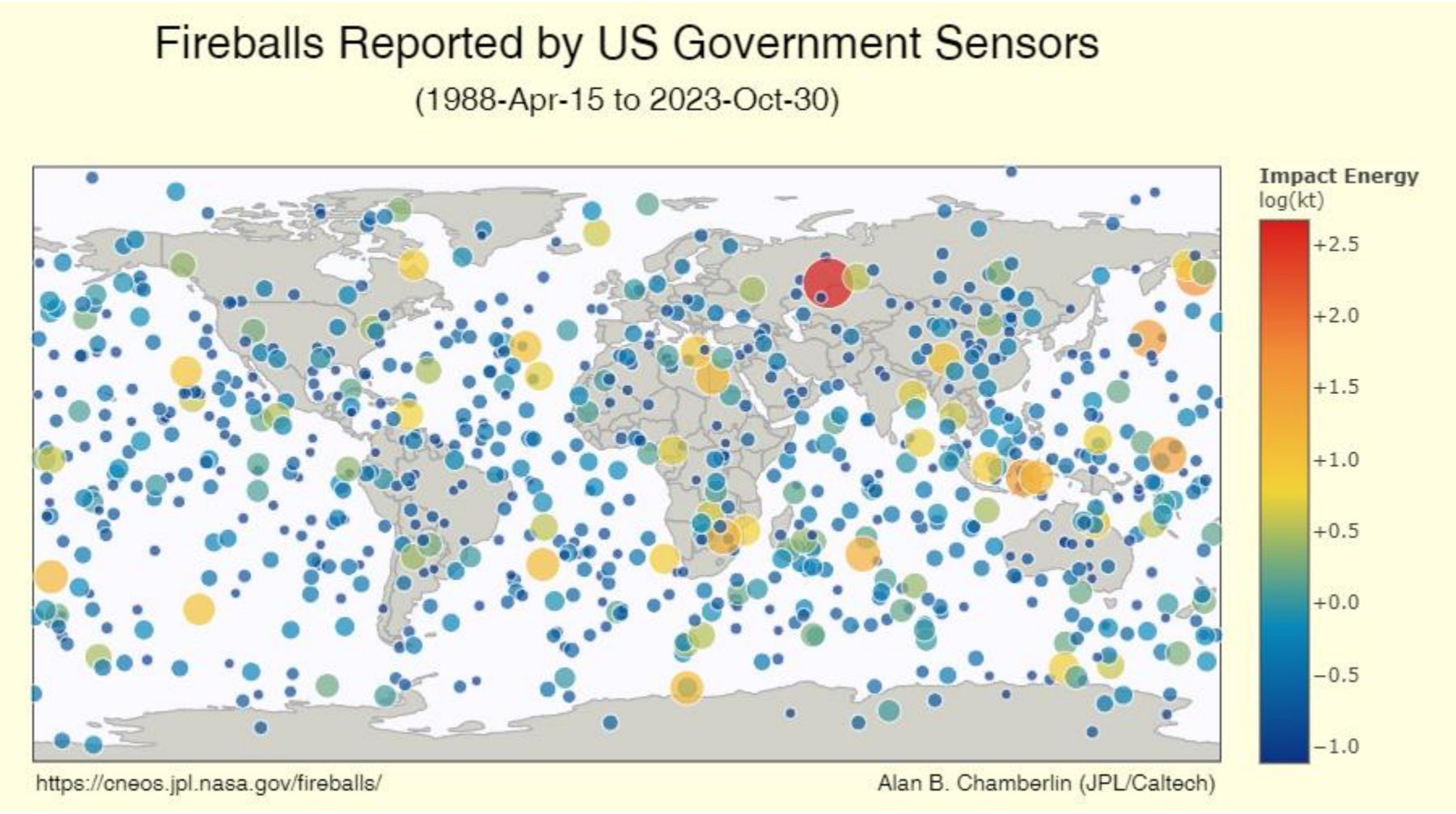

Small bodies continuously bombard the Earth's atmosphere.

According to NASA's CNEOS data center, there is an event detectable by military satellites on average **every two weeks**, with a **mean diameter of about 1-2 m**.

About 9.8% of the events belong to **Jupiter Family Comets**, while 85.5% have a Tisserand parameter with respect to Jupiter, **typical of asteroid orbits**.

There are **no known meteorites of cometary origin**.

NEAs impact list

List of near-Earth asteroids discovered a few hours before the collision with Earth in order of date. The estimated diameter D comes from the absolute magnitude value. The Minor Planet Electronic Circulars (MPEC) from the Minor Planet Centre are listed for each asteroid.

Designation	Meteorites	Impact date	UTC	Discoverer	Survey	Code	D (m)
2008 TC3[a]	Y	2008-10-07	02:46	Richard Kowalski	Mount Lemmon Survey	G96	3-4
2014 AA[b]	N	2014-01-02	02:33 ($\pm$1 h)	Richard Kowalski	Mount Lemmon Survey	G96	3
2018 LA[c]	Y	2018-06-02	16:44	Richard Kowalski	Mount Lemmon Survey	G96	3-4
2019 MO[d]	N	2018-06-22	21:25	—	ATLAS-MLO	T08	4-6
2022 EB5[e]	N	2022-03-11	21:22	Krisztián Sárneczky	Konkoly Observatory	K88	2
2022 WJ1[f]	N	2022-11-19	08:27	David Rankin	Mount Lemmon Survey	G96	1
2023 CX1[g]	Y	2023-02-13	02:59	Krisztián Sárneczky	Konkoly Observatory	K88	1
2024 BX1[h]	Y	2024-01-21	00:32	Krisztián Sárneczky	Konkoly Observatory	K88	1
2024 RW1[i]	N	2024-09-04	16:39	Jacqueline Fazekas	Mount Lemmon Survey	G96	1.5

[a] MPEC 2008-T72, https://minorplanetcenter.net/mpec/K08/K08T72.html
[b] MPEC 2014-A02, https://minorplanetcenter.net/mpec/K14/K14A02.html
[c] MPEC 2018-L04, https://minorplanetcenter.net/mpec/K18/K18L04.html
[d] MPEC 2019-M72, https://minorplanetcenter.net/mpec/K19/K19M72.html
[e] MPEC 2022-E178, https://minorplanetcenter.net/mpec/K22/K22EH8.html
[f] MPEC 2022-W69, https://minorplanetcenter.net/mpec/K22/K22W69.html
[g] MPEC 2023-C103, https://minorplanetcenter.net/mpec/K23/K23CA3.html
[h] MPEC 2024-B76, https://minorplanetcenter.net/mpec/K24/K24B76.html
[i] MPEC 2024-R68, https://minorplanetcenter.net/mpec/K24/K24R68.html

Asteroid Orbits and Impact Parameters

Table 5

Impact parameters at 100 km altitude (WGS84 ellipsoid) from Earth surface of 2023 CX1 and 2024 BX1, with their 1-σ uncertainties. The velocity is given with respect to the ground. Elevation is the angle that the velocity vector forms with the ground; the module corresponds to the inclination of the trajectory. The azimuth gives the direction of the velocity vector seen by the observer on Earth, so to get the incoming direction, we must add 180 degrees.

Object	2023 CX1	2024 BX1
Time (UTC)	2023-02-13 02:59:13.387 ± 0.070 s	2024-01-21 00:32:37.712 ± 0.069 s
Latitude (deg)	49.919022 ± 0.00012	52.584477 ± 0.000176
East Longitude (deg)	-0.1467625 ± 0.0006545	12.356914 ± 0.000376
Velocity (km s^{-1})	14.01645 ± 0.000185	15.197428 ± 0.000266
Elevation (deg)	-49.153055 ± 0.00051	-75.605503 ± 0.000293
Azimuth (deg)	101.386628 ± 0.000393	73.846168 ± 0.000300
1-σ semi-major axis (m)	95.93	63.88
1-σ semi-minor axis (m)	14.23	6.12

Table 6

Keplerian orbital elements of 2008 TC3, with the corresponding epoch, expressed in MJD, and impact parameters at 100 km altitude from Earth's surface. Errors refer to the 1-σ formal uncertainties.

Orbital Data	Value	Impact Parameter	Value
Epoch (MJD)	54745.8110 TDT	Time (UTC)	2008-10-07 02:45:30.09 ± 0.14 s
Semi-major axis (au)	1.284115 ± 0.000011	Latitude (deg)	21.0884 ± 0.0009
Eccentricity	0.294852 ± 0.000007	East Longitude (deg)	30.5347 ± 0.0038
Inclination (deg)	2.403189 ± 0.000057	Velocity (km s^{-1})	12.38041 ± 0.00005
Longitude of node (deg)	194.11280 ± 0.00000282	Elevation (deg)	-20.8360 ± 0.0030
Argument of perihelion (deg)	234.0469348 ± 0.000087	Azimuth (deg)	101.0953 ± 0.0015
Mean anomaly (deg)	329.66890 ± 0.00052	1-σ semi-major axis (m)	610
Normalized RMS	0.000	1-σ semi-minor axis (m)	98

Important parameters for the model

Fragments sample

A priori, we do not know the masses of the fragments in the strewn field, i.e. the meteorites' masses. So, in our model, we assume the following **final masses** with spherical shape: **1, 0.3, 0.2, 0.1, 0.05, 0.02, 0.005 and 0.001 kg**. So, we use some "sample" particles to show the **final strewn field's possible range and position**. With good approximation, these masses for the fragments correspond to the typical masses of meteorites on the ground.

Strength

In the case of the major fireballs observed by the European Fireball Network, the strength of the first fragmentation is in the 0.4-4 MPa range, while the main fragmentation is in the 3.5-12 MPa range. In our model, as it is constructed, we only have one fragmentation, and we use some test values for the strength: the first with S **≈ 1 MPa** and the second with S **≈ 5 MPa**, with an extension toward S **≈ 0.5 MPa** in some cases.

Atmospheric profile

A good atmospheric profile is one of the critical points, along with the value of strength, for computing a realistic strewn field. The essential quantities it must report are the **air density** ρ_a at different heights (or the pressure and temperature from which the density can be computed) and the **speed and direction of the wind** W.

Masses distribution

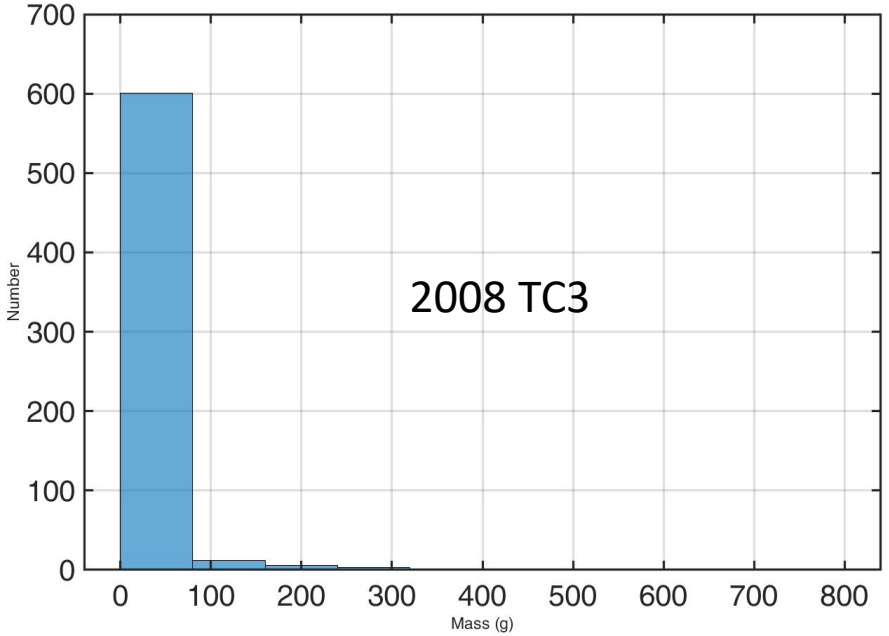

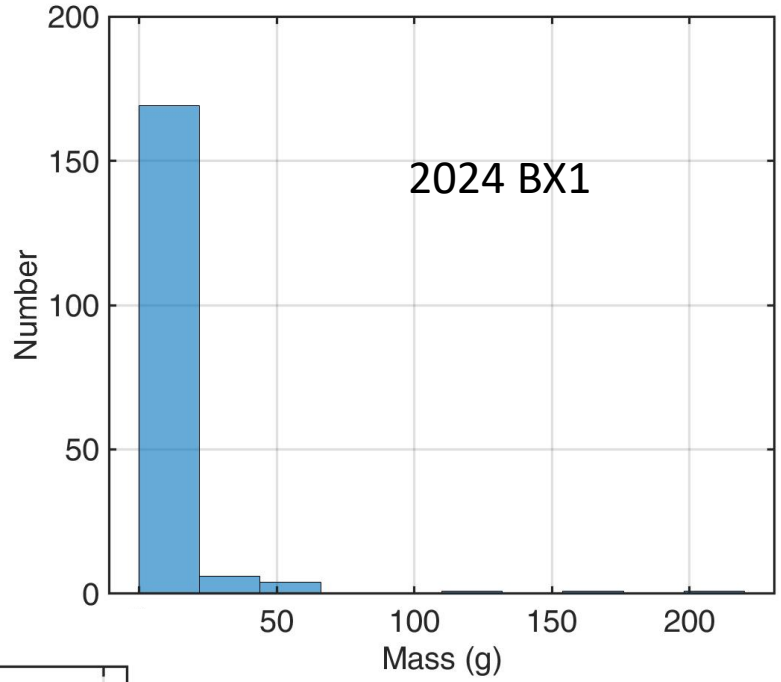

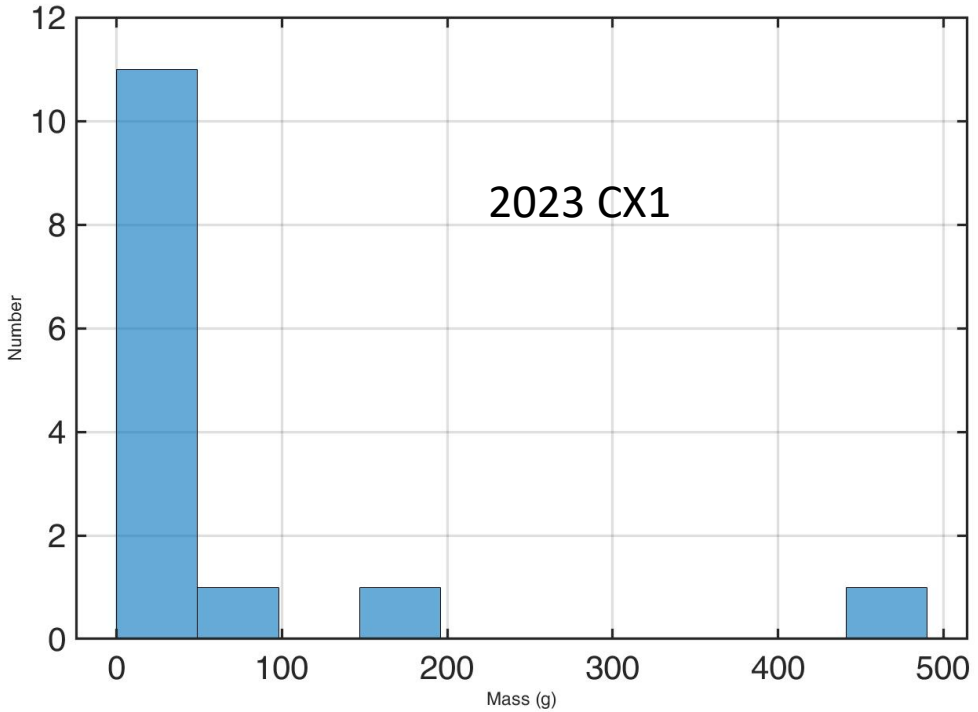

2024 BX1 model

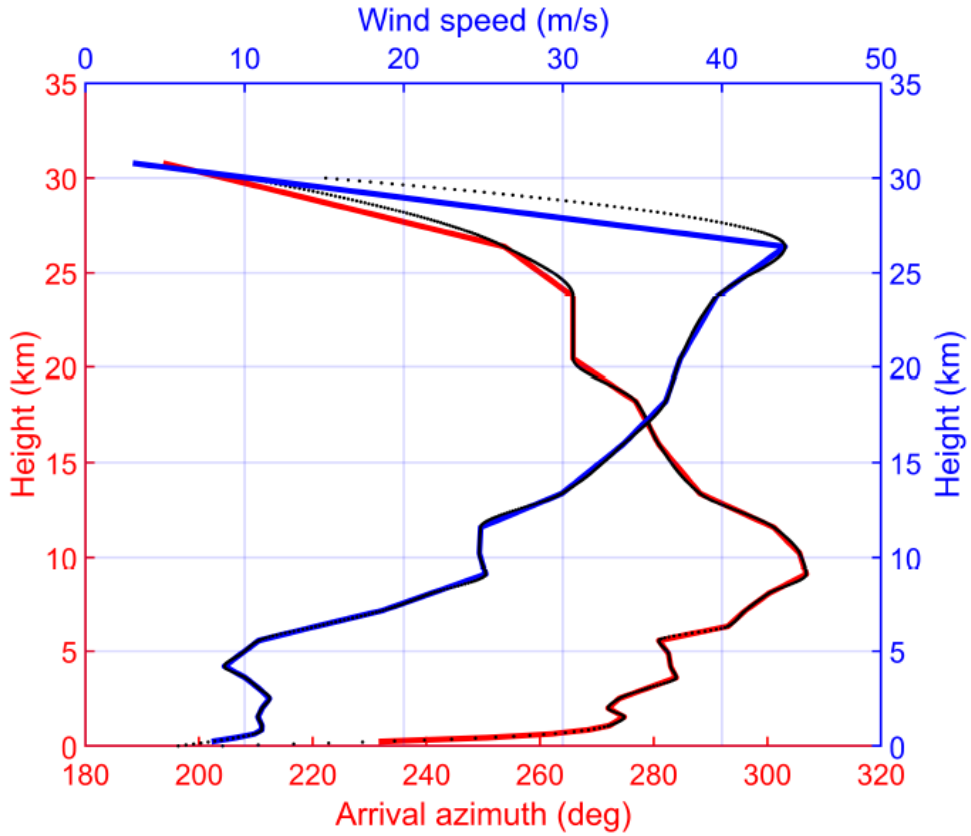

Figure 3: The atmospheric profile used for the 2024 BX1 event, computed by Meteo Expert for 24 January 2024, 00 UTC at Lat. 52.6331° N and Long. 12.6379° E, a point near the start of the dark flight phase. The modulus of the wind speed (m/s) and the arrival azimuth of the wind (deg) are shown. The dotted line interpolates the data provided by the atmospheric profile using a shape-preserving piecewise cubic interpolation.

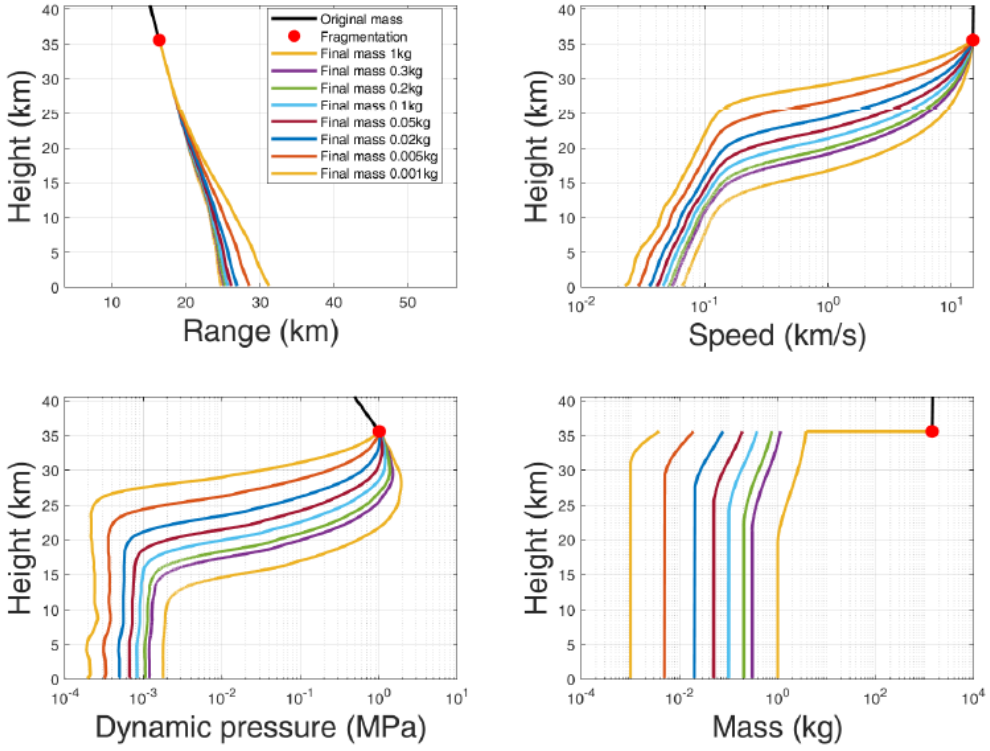

Figure 7: The results of the fragmentation model for the 2024 BX1 fall with $S \approx 1$ MPa and the Meteo Expert atmospheric profile. The different colours refer to the assumed fragments to sample the strewn field. In the height vs mass plot, note that the fragment masses are subject to a residual ablation after fragmentation. For more readability, some scales in the graphs are logarithmic.

Strewn field Ribbeck meteorite

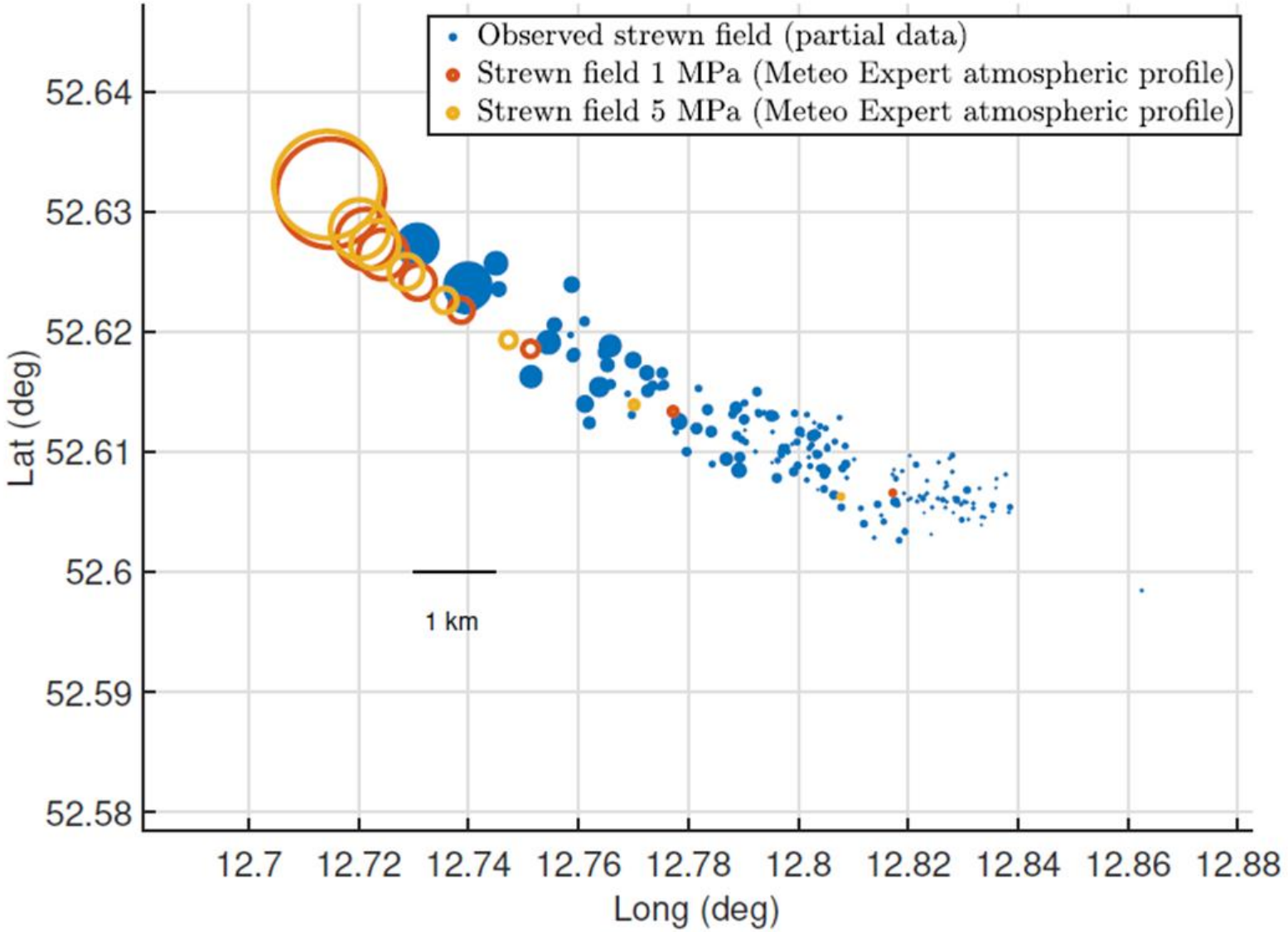

Figure 8: A comparison between the observed strewn field of 2024 BX1 fall from Bischoff et al. (2024) and the two theoretical ab initio strewn fields with a mean strength of 1 and 5 MPa. This figure shows the positions of the 185 meteorites of 202 recovered, whose positions are known. The circles are proportional to the mass of the recovered meteorite, and the agreement is slightly better for the strewn field with $S \approx 1$ MPa; see Table 7 for a numerical comparison.

2023 CX1 model

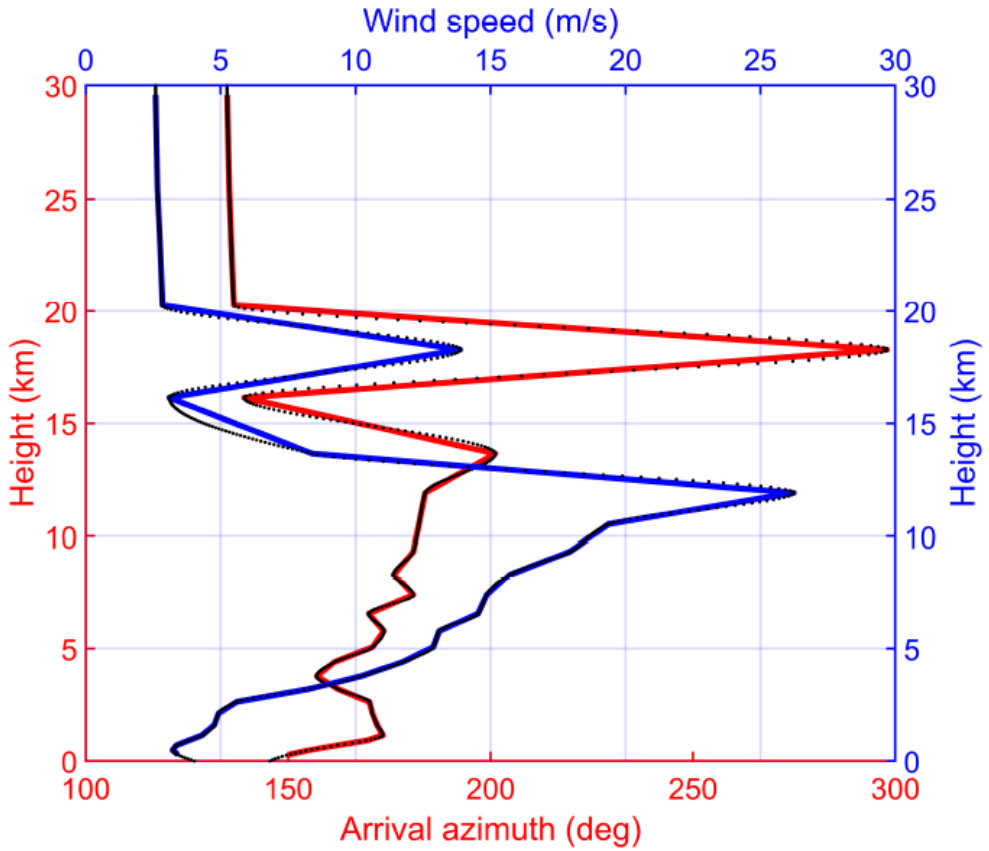

Figure 2: The atmospheric profile used for the 2023 CX1 event, computed by Meteo Expert for 13 February 2023, 03 UTC at Lat. 49.7979° N and Long. 0.7533° E, a point near the start of the dark flight phase. The modulus of the wind speed (m/s) and the arrival azimuth of the wind (deg) are shown. The dotted line interpolates the data provided by the atmospheric profile using a shape-preserving piecewise cubic interpolation.

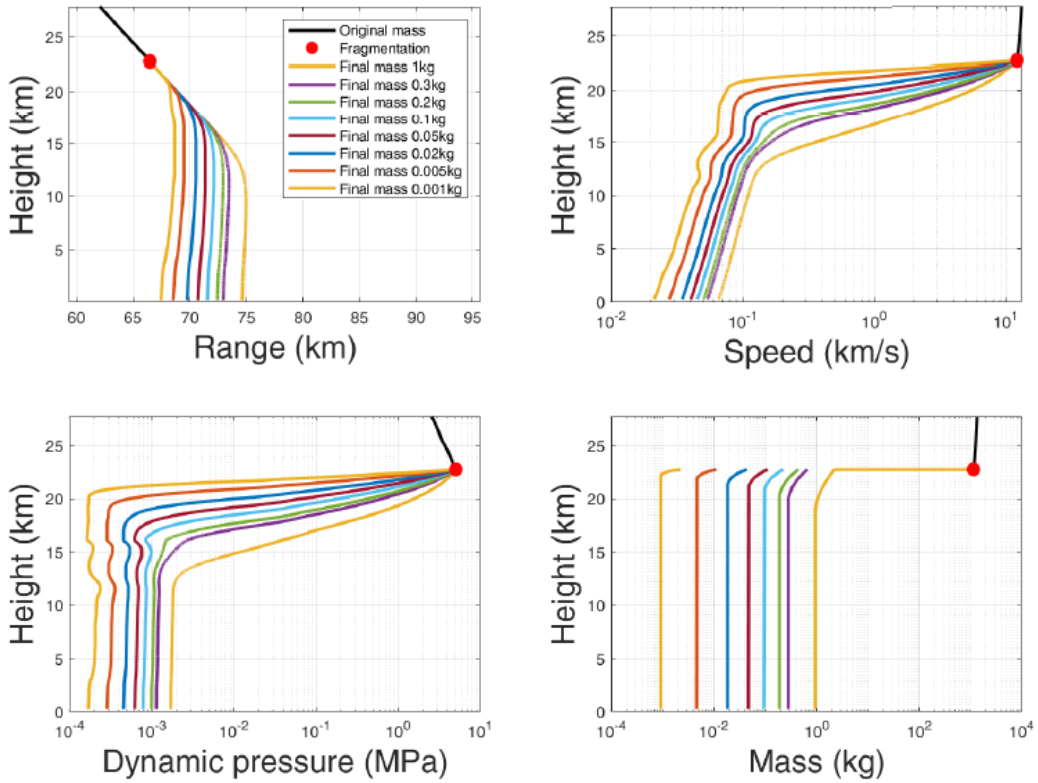

Figure 5: The results of the fragmentation model for the 2023 CX1 fall with $S \approx 5$ MPa and the Meteo Expert atmospheric profile of 03 UTC. The different colours refer to the assumed fragments to sample the strewn field. In the height vs mass plot, note that the fragment masses are subject to a residual ablation after fragmentation. For more readability, some scales in the graphs are logarithmic.

Strewn field Saint-Pierre-le-Viger meteorite

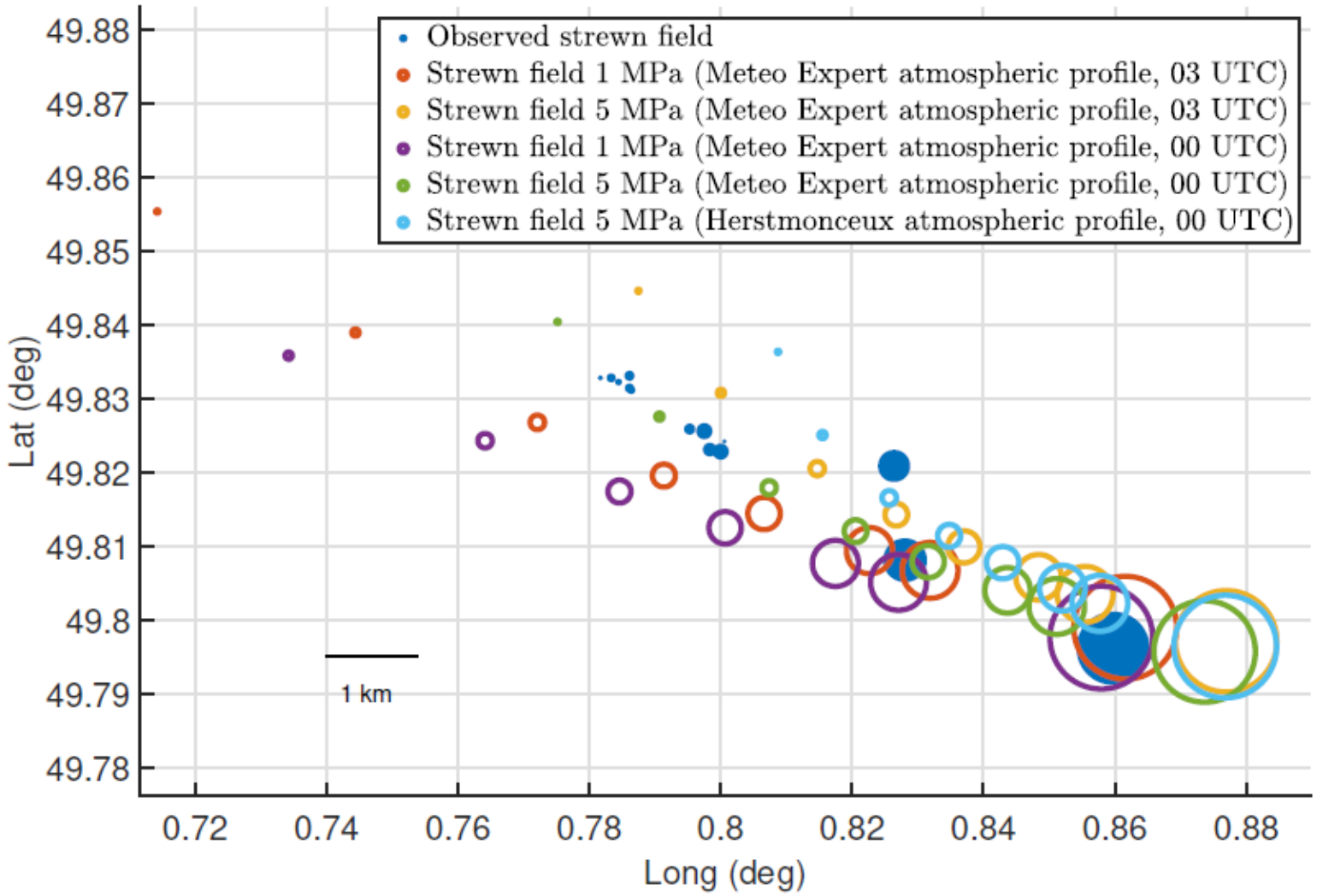

Figure 6: A comparison between the observed strewn field of 2023 CX1 fall from Table 2 and the theoretical ab initio strewn field with mean strengths of 1-5 MPa and the Meteo Expert atmospheric profile. The circles are proportional to the mass of the recovered meteorite, and as a comparison, the strewn field with the Herstmonceux data is also present. As we can see, the fit is better for $S \approx 5$ MPa with the Meteo Expert atmospheric profile, see Table 7 for a numerical comparison. Coincidentally, the atmospheric profile with strength 5 MPa at 00 UTC provides slightly better results than that at 03 UTC.

2008 TC3 model

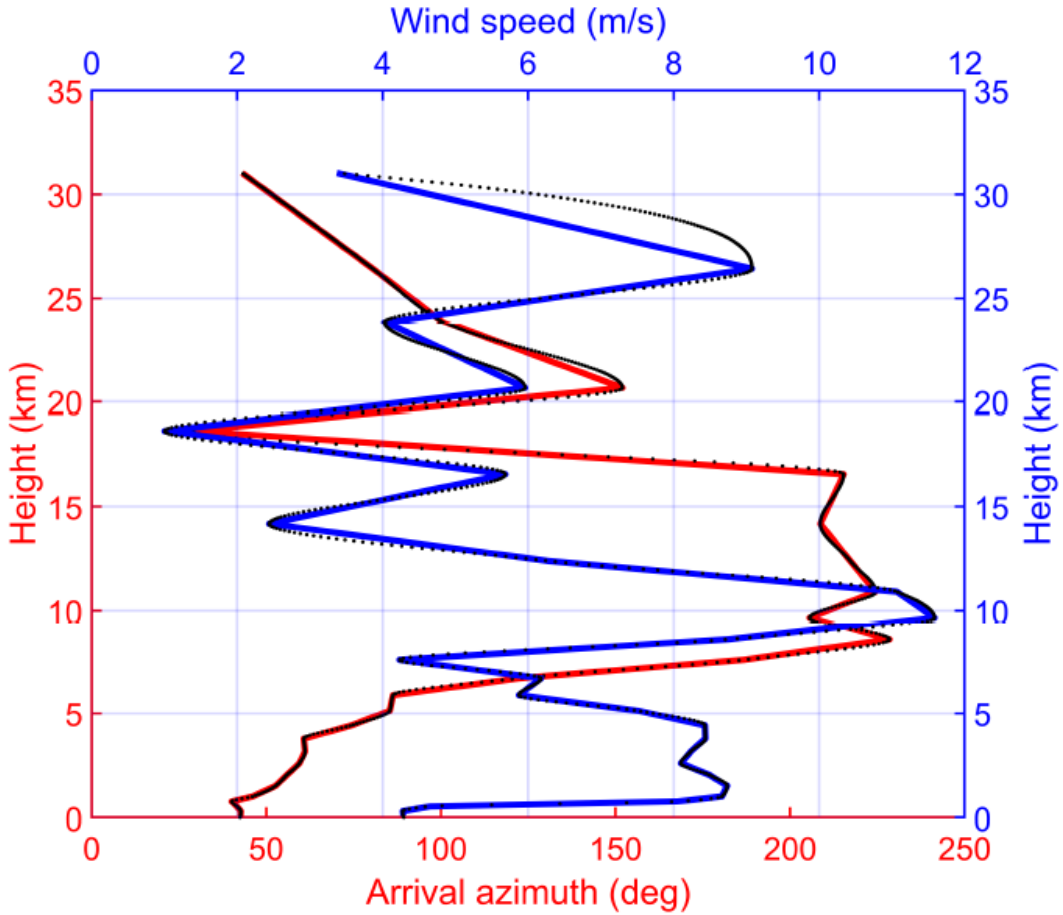

Figure 10: The atmospheric profile used for the 2008 TC3 event, computed by Meteo Expert for 7 October 2008, 03 UTC at Lat. 20.97° N and Long. 32.16° E. As in the previous atmospheric profile, the modulus of the wind speed (m/s) and the arrival azimuth of the wind (deg) are shown. The dotted line interpolates the data provided by the atmospheric profile using a shape-preserving piecewise cubic interpolation.

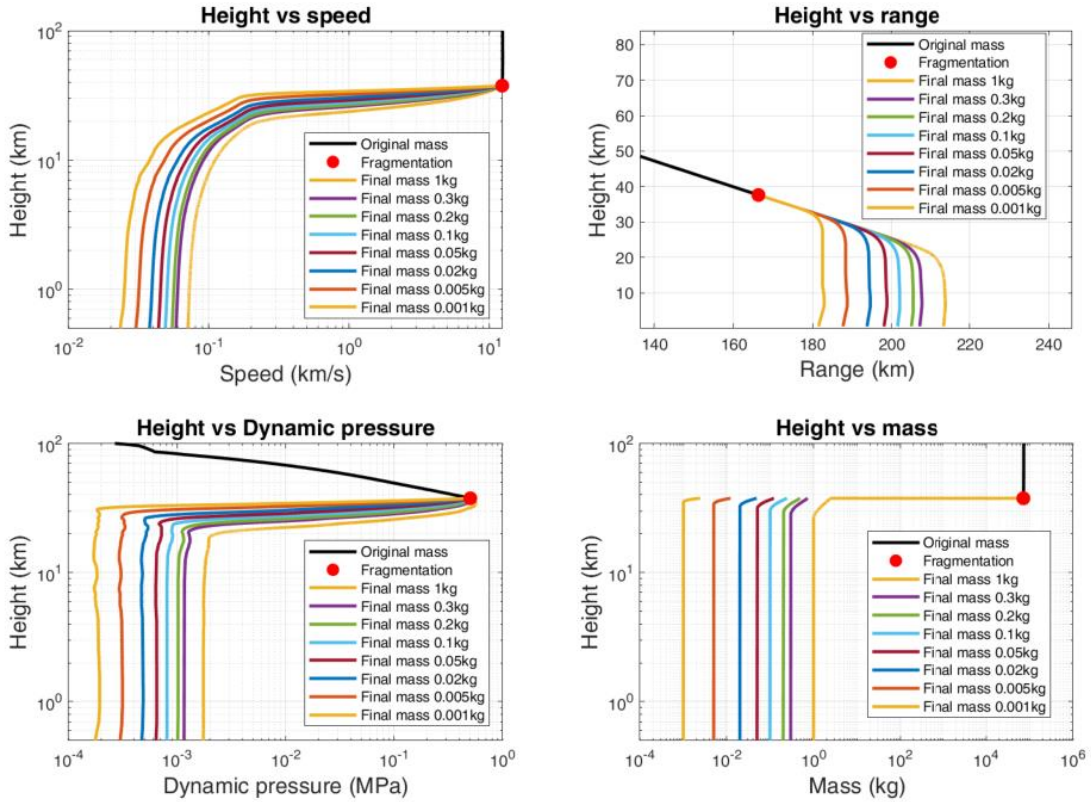

2008 TC3 fragmentation model with S=0.1 MPa

Strewn field Almahata Sitta meteorite

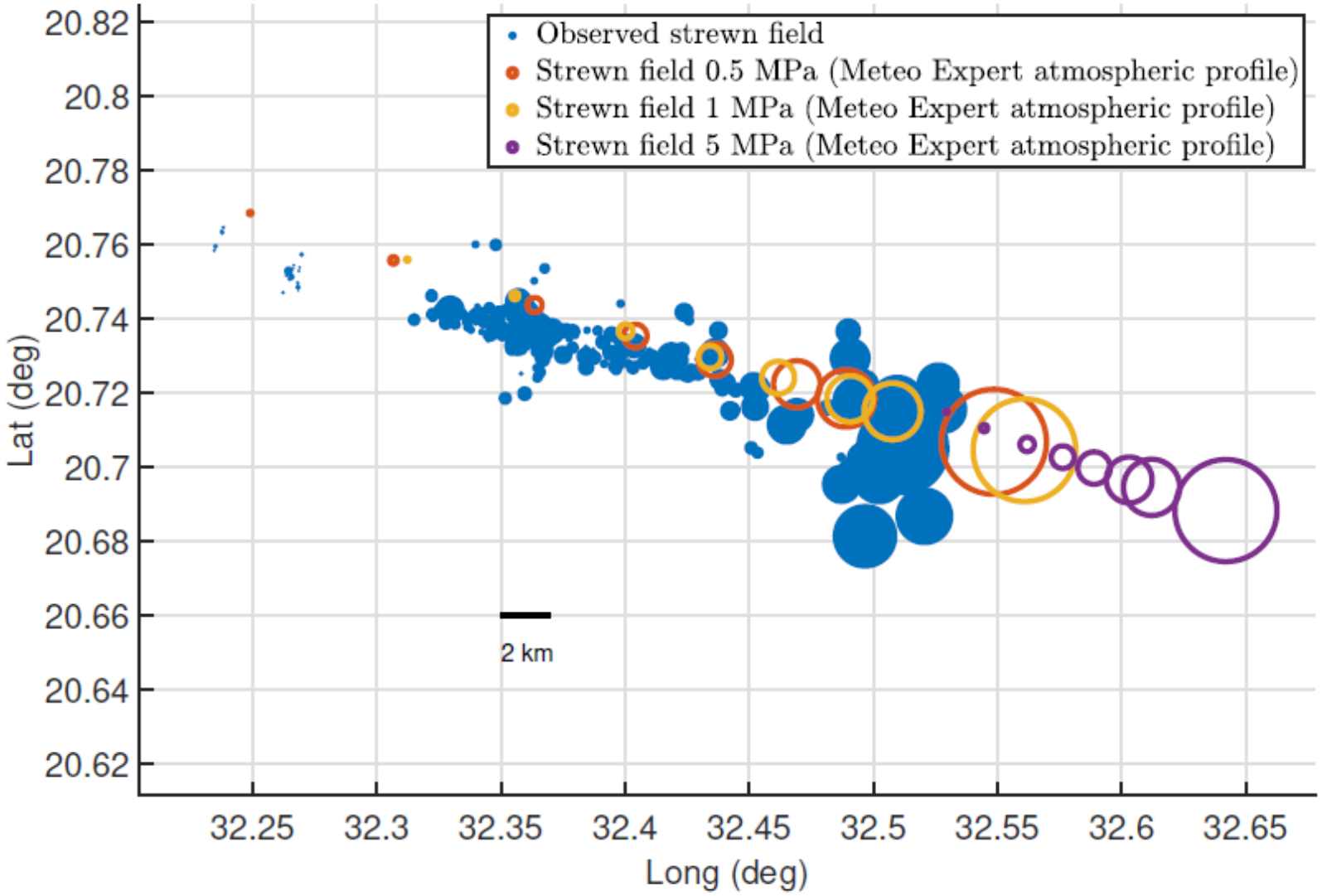

Figure 9: A comparison between the observed strewn field of 2008 TC3 with 624 meteorites of known position and the three theoretical ab initio strewn fields with a mean strength of 0.5, 1 and 5 MPa. The circles are proportional to the mass of the recovered meteorite; as we can see, the agreement is qualitatively better for the strewn field with $S \approx 0.5$ MPa, but also for $S \approx 1$ MPa, the result appears good, see Table 7 for a numerical comparison.

Table 7

The RMS values for 2023 CX1, 2024 BX1 and 2008 TC3, computed between the best-fit curve of the theoretical strewn field, characterised by the mean strength S with the atmospheric profile, and the observed positions of the meteorites, regardless of mass. ME=Meteo Expert, H=Herstmonceux. For 2023 CX1, the agreement observed-computed strewn field is better for $S \approx 5$ MPa; for 2024 BX1, the best is for $S \approx 1$ MPa, while for 2008 TC3 is better for $S \approx 0.5$ MPa. **The values in brackets refer to the pancake model. As we can see, there is no significant difference between the fragmentation and pancake models. However, the fragmentation model values are slightly lower or equal, except for one value in the 2023 CX1 column referring to the ME atmospheric profile at 03 UTC with strength 1 MPa.**

2023 CX1	RMS (km)	2024 BX1	RMS (km)	2008 TC3	RMS (km)
ME (1 MPa; 00 UTC)	1.26 (1.24)	ME (1 MPa; 00 UTC)	0.56 (0.71)	ME (0.5 MPa; 03 UTC)	1.1 (1.2)
ME (5 MPa; 00 UTC)	0.29 (0.29)	ME (5 MPa; 00 UTC)	0.89 (0.90)	ME (1 MPa; 03 UTC)	1.7 (2.1)
ME (5 MPa; 03 UTC)	0.74 (0.77)	-	-	ME (5 MPa; 03 UTC)	17.8 (18.4)
ME (1 MPa; 03 UTC)	0.84 (0.82)	-	-	-	-
H (5 MPa; 00 UTC)	1.4 (1.5)	-	-	-	-

The strewn field of 2022 WJ1: where are the meteorites?

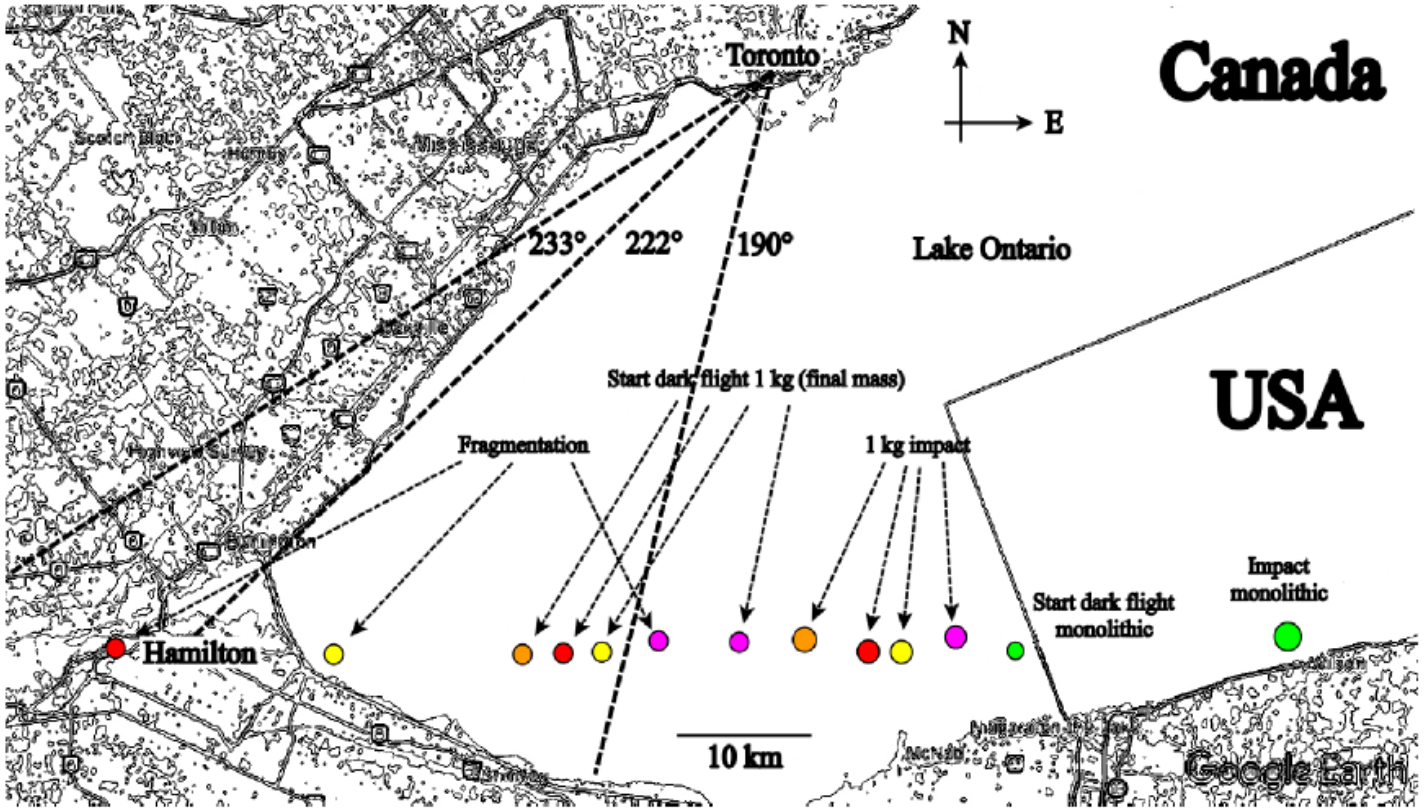

Figure 16: This drawing based on a Google Earth image shows the fragmentation position, start dark flight and impact points for 2022 WJ1. To avoid a drawing that is too complex to see, the impact points are those of the fragments with a final mass of 1 kg. Fragments of lesser mass fall first, and fragments of greater mass fall after this point. In any case, they remain aligned in the same east-west direction. The colours indicate different strengths: orange 0.1 MPa, red 0.5 MPa, yellow 1 MPa, pink 3 MPa and green 5 MPa. Also shown are the lines of sight from the EarthCam. The fragmentation for $S = 0.1$ MPa is outside the drawing on the left.

Conclusions

(1) Despite the approximations used in the fragmentation model, which considers a **single fragmentation** followed by a **release of fragments of different mass**, all with the **same speed and direction** with no lateral speed component, the results of the computed strewn field from orbital elements appear pretty good.

(2) This weak dependence on the fragmentation number is probably caused by the **asteroid's wake vacuum region**, which **retains the smaller fragments that break off in the secondary fragmentations** until reaching the **main fragmentation** of the body when the **containment effect ceases**, so all the fragments are free to fall independently.

(3) A weak point of our procedure is the **lack of a priori knowledge of the asteroid's strength**, which is a **very important parameter** (**with atmospheric profile**) because it determines the height of the fragmentation, so the length of the fragment's path before reaching the ground. This forces us to adopt a range of reasonable values, which may be good for most cases but may not always be valid.

(4) The values of the **other parameters** adopted for the model are **less critical than strength** because they determine the **ablation rate and the drag**. The asteroid's diameter can be estimated from telescope observations, so it is a secondary factor for the position of the strewn field. Overall, **the fixed parameter values adopted in the text are generic enough to describe most falls**.


THANK YOU FOR YOUR ATTENTION!